https://doi.org/10.7840/kics.2024.49.11.1525

Hybrid Precoding Optimization Based on Quantum Neural Network for Multi-User MISO Systems

Adriansyah Dwi Rendragraha•, Soo Young Shin°

ABSTRACT

Hybrid precoding emerges as a promising solution for minimizing hardware costs and power consumption while maintaining near-optimal performance for multi-user (MU) multiple-input-single-output (MISO) communication. It leverages an extensive array of phase shifters to execute high-dimensional analog precoding, addressing significant path loss, alongside a limited number of radio frequency chains for low-dimensional digital precoding. This paper introduces a novel approach to hybrid precoding optimization employing Quantum Neural Networks (QNN) and an unsupervised learning technique, with the objective to maximize spectral efficiency and reducing the complexity. The QNN is utilized to obtain optimal analog precoding matrix, which is then utilized to calculate digital precoding using zero-forcing criteria. Simulation results demonstrate the spectral efficiency of QNN-based hybrid precoding gain improvement compared to other hybrid precoding solutions with low complexity.

Key Words : Hybrid precoding, quantum neural networks, unsupervised learning, wireless communication

Ⅰ. Introduction

The millimeter-wave (mmWave) has emerged as a promising solution[1] for addressing spectrum congestion issues due to its massive available frequency bands for wireless communications, yet propagation at the highest frequencies faces a significant large path loss. This challenge can be mitigated by leveraging precoding techniques from multiantenna transceivers to increase spectrum efficiency.

Digital precoding provides more flexibility when all signal processing is performed. Nonetheless, it requires a radio frequency (RF) chain, a digital-to-analog converter (DAC), and an analog-to-digital converter (ADC) for each antenna element, leading to hardware costs and power consumption. This becomes particularly burdensome in scenarios involving large antenna arrays. Hence, the hybrid precoding architecture emerges as a promising alternative[2-6]. It leverages an extensive array of phase shifters to execute high-dimensional analog precoding, addressing significant path loss, alongside a limited number of radio frequency chains for low-dimensional digital precoding. This hybrid approach provides a near-optimal solution compared to digital precoding and the requisite flexibility for advanced multiplexing and multiuser techniques while mitigating hardware costs and power consumption.

In hybrid precoding, there are two types of analog precoding structures. First is a fully-connected struc-

※ This work was supported by the National Research Foundation of Korea(NRF) grant funded by the Korea government. (MSIT) (No.2022R1A2B5B01001994) This work was supported by Institute of Information & communications Technology Planning & Evaluation (IITP) grant funded by the Korea government(MSIT) (No. 2021-0-02120, Research on Integration of Federated and Transfer learning between 6G base stations exploiting Quantum Neural Networks).
• First Author : Kumoh National Institute of Technology, Department of IT Convergence Engineering, 220116147@kumoh.ac.kr, 학생회원
° Corresponding Author : Kumoh National Institute of Technology, Department of IT Convergence Engineering, wdragon@kumoh.ac.kr, 종신회원
논문번호 : 202405-098-B-RE, Received May 13, 2024; Revised June 26, 2024; Accepted July 19, 2024

ture as shown in Figure 1a where all RF chains are connected to all antenna elements and the second structure, shown in Figure 1b, adopts a sub-connected design in where each RF chain connects solely to a subset of antenna elements. Various approaches and techniques have been produced surrounding the optimization of hybrid precoding. In [2], the spatial structure of the mmWave channel is utilized to design the digital and analog precoding as a sparse reconstruction problem via orthogonal matching pursuit (OMP) to improve spectral efficiency. The trade-off shown in the high computational complexity while the performance can approach the unconstrained performance limits. Reference [3] used zero-forcing precoding considering quantized analog and digital precoding for fully-connected and sub-connected structures. By utilizing the channel correlation-based codebook, the sub-connected structure continuously surpasses the fully connected structure in massive MIMO or low signal-to-noise ratio scenarios with the assumption the

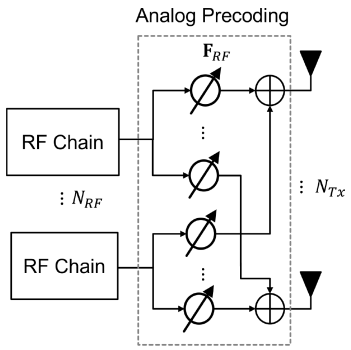

(a) Fully-connected.

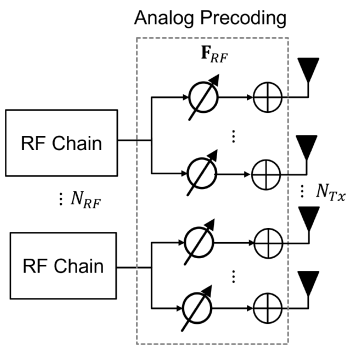

(b) Sub-connected.

Fig. 1. Analog precoding structure in hybrid precoding.

system operates in a low-mobility scenario with a large channel block length. Other work[4], proposed a Kalman-based hybrid precoding scheme, where the baseband precoding matrix is considered as the state matrix in Kalman formulation. The Kalman algorithm utilizing a special designed error formulation, a two-step process is implemented: first, the RF precoding/combining matrix is calculated, followed by the design of the digital baseband precoder at the base station (BS). Although it is claimed to have affordable complexity, no complexity analysis is provided to support the assertion.

Moreover, neural networks (NN) have shown potential for solving complex nonconvex optimization like hybrid precoding optimization[5,6]. In [5], unsupervised NN with imperfect channel state information (CSI) is utilized to improve the achievable sum rate. The purpose of employing unsupervised learning is to reduce training time and cost, thus the estimated channel data for training can be used directly without obtaining the optimal solution. Given that the results demonstrate it's better than the traditional method, a comparison with other NN models can be provided. In [6], used an attention-based hybrid precoding approach to maximize the achievable sum rate while reducing the complexity. The attention layer is used to get inter-user interference features from input data and the convolutional neural network (CNN) layer to design the optimized analog precoding.

Furthermore, there are studies[7,8] that have explored the development of NN and quantum computing as quantum neural networks (QNN). QNN is a subclass within variational quantum algorithms (VQA), where the networks are constructed using quantum circuits that incorporate parameterized gate operations[9]. Initially, information is encoded into a quantum state through a process known as a state preparation routine or feature map[10]. Once the data is successfully encoded into the quantum state, the gates are adjusted and optimized to perform a specific task, which typically involves minimizing a loss function. The optimization process iteratively refines the parameters of the quantum gates to improve the model performance. The final output of the quantum

model is then derived by applying a classical post-processing function to the measurement outcomes obtained from the quantum circuit. QNN can offer a speedup process based on quantum entanglement and superposition, also reducing complexity by leveraging quantum computation. Several studies have already utilized this QNN advantage for wireless communication optimization[11-13].

In this paper, a QNN-based optimization for MUMISO hybrid precoding with an unsupervised learning approach is proposed to maximize the spectral efficiency and lowering the complexity. The QNN used to obtain the optimized analog precoding that later used to calculate digital precoding based on zero-forcing criteria. The main contributions of this paper are:

- Employs QNN for hybrid precoding optimization to enhance spectral efficiency and lower complexity.
- Unsupervised learning is considered in this study to avoid the lack of reference points, i.e., data labels.
- Represent the optimization problem that will be solved by quantum-based optimization.
- The simulation result is presented to evaluate the proposed method.

The remaining sections of the paper are structured as follows: The scenario of system model is introduced in Section II. Followed by section III, discusses the quantum-based approach is covered. Section IV summarizes the experimental results of this paper. The paper is finally concluded in Section V.

Notations: Bold italic lowercase and bold uppercase letters denote vectors and matrices, respectively. $(\cdot)^{-1}$, $(\cdot)^{H}$, and $(\cdot)^{T}$ indicate the inverse, hermitian, and transpose operation. Let $|\cdot|$ and $\|\cdot\|_f$ denotes absolute values and frobenius norm operation. The $\otimes$ denote knocker product operation. Let $\mathbf{R_y}$, $\mathbf{C_z}$ and $\mathcal{H}$ represents as operation of rotation on the Y axis, Controlled-Z gate operation, and Hadamard gate.

Ⅱ. System Model

Consider a downlink scenario with MU-MISO system, which includes one base station (BS) that serves K single antenna users with fully-connected architecture of hybrid precoding as presented in Figure. 2. The BS consists of N_{Tx} transmit antennas and N_{RF} radio frequency chain. The total data streams N_{s} being transmitted is equal to K. By adopting a narrowband block-fading channel model[2,14], the received signal model $\mathbf{y}$ for all K users is given as

$$\mathbf{y} = \mathbf{H}\mathbf{F}_{\mathrm{RF}}\mathbf{F}_{\mathrm{BB}}\boldsymbol{s} + \boldsymbol{n}, \tag{1}$$

where $\mathbf{H} = [h_1, \ldots, h_K]^T \in \mathbb{C}^{K\times N_{\mathrm{Tx}}}$ is channel matrix; $\mathbf{F}_{\mathrm{RF}} \in \mathbb{C}^{N_{\mathrm{Tx}}\times N_{\mathrm{RF}}}$ is analog precoding matrices; $\mathbf{F}_{\mathrm{BB}} = [f_{\mathrm{BB},1}, \ldots, f_{\mathrm{BB},N_s}] \in \mathbb{C}^{N_{\mathrm{RF}}\times N_{\mathrm{s}}}$ is digital precoding matrices; $s \in \mathbb{C}^{N_{\mathrm{s}}\times 1}$ is transmitted signal vector, satisfying $\mathbf{E}[ss^H] = \frac{\rho}{K}\mathbf{I}_K$, which ρ is transmitted power assume equally allocated among different users; and $n \in \mathbb{C}^{K\times 1}$ is noise. Assuming that the channel $\mathbf{H}$ is perfectly known for the transmitter[2,4]. In practical, the compressive sensing (CS) based schemes to estimate the channel $\mathbf{H}$ with reduced pilot can be applied in hybrid precoding scenarios, such as the OMP algorithm[14]. Additionally, deep learning (DL) based channel estimation approach[15] can also be employed in hybrid precoding scenario[6].

The Saleh-Valenzuela channel model is utilized, employing a uniform linear array (ULA)[14] antenna as the channel matrix is presented by

$$\boldsymbol{h}_k = \sqrt{\frac{N_{\mathrm{Tx}}N_{\mathrm{Rx}}}{N_{\mathrm{path}}}}\sum_{l=1}^{N_{\mathrm{path}}}\beta_l \mathbf{A}_{\mathrm{Rx}}^{k}(\phi^{\mathrm{Rx}})\mathbf{A}_{\mathrm{Tx}}^{k}(\phi^{\mathrm{Tx}})^H, \tag{2}$$

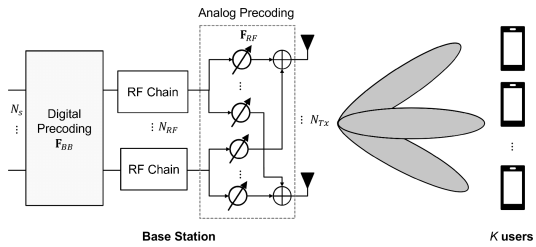

Fig. 2. Hybrid precoding with fully-connected architecture.

where the following distributions are assumed $\beta_l \sim \mathcal{CN}(0,1)$, $\phi^{\mathrm{Rx}} \sim \mathcal{N}(0,2\pi)$ and $\phi^{\mathrm{Tx}} \sim \mathcal{N}(0,2\pi)$ to be the complex path gain, angle of departure and angle of arrival (AoD and AoA), respectively. The Npath is the number of paths. Since ULA are assigned at the base station and users, the $\mathbf{A}_{\mathrm{Tx}}$ ($\phi^{\mathrm{Tx}}\phi$) and $\mathbf{A}_{\mathrm{Rx}}$ (ϕ^{Rx}) as corresponding antenna steering vectors of transmitter and receiver can be stated as

$$\mathbf{A}_{\mathrm{Tx}}(\phi^{\mathrm{Tx}}) = \frac{1}{\sqrt{N_{\mathrm{Tx}}}}\left[1, e^{-j\frac{2\pi}{\lambda}d\cos(\phi^{\mathrm{Tx}})}, \ldots, e^{-j\frac{2\pi}{\lambda}d(N_{\mathrm{Tx},k}-1)\cos(\phi^{\mathrm{Tx}})}\right]^T, \tag{3}$$

$$\mathbf{A}_{\mathrm{Rx}}(\phi^{\mathrm{Rx}}) = \frac{1}{\sqrt{N_{\mathrm{Rx}}}}\left[1, e^{-j\frac{2\pi}{\lambda}d\cos(\phi^{\mathrm{Rx}})}, \ldots, e^{-j\frac{2\pi}{\lambda}d(N_{\mathrm{Rx},k}-1)\cos(\phi^{\mathrm{Rx}})}\right]^T, \tag{4}$$

where $d = \frac{\lambda}{2}$ and λ denotes distance between each antenna and the signal wavelength. The spectral efficiency calculation R[4,6] is presented as

$$R = \mathbb{E}\left[\frac{1}{K}\sum_{k=1}^{K}\log_2\left(\frac{\gamma|\boldsymbol{h}_k\mathbf{F}_{\mathrm{RF}}\boldsymbol{f}_{\mathrm{BB},k}|^2}{\sigma^2+\gamma\sum_{q\neq k}|\boldsymbol{h}_k\mathbf{F}_{\mathrm{RF}}\boldsymbol{f}_{\mathrm{BB},q}|^2}\right)\right], \tag{5}$$

where γ indicate signal-noise-ratio. The optimization problem of hybrid precoding ($\mathbf{F}_{\mathrm{RF}}$ and $\mathbf{F}_{\mathrm{BB}}$) is expressed as

$$\begin{aligned} \max_{\mathbf{F}_{\mathrm{RF}},\mathbf{F}_{\mathrm{BB}}} \quad & R(\mathbf{H},\mathbf{F}_{\mathrm{RF}},\mathbf{F}_{\mathrm{BB}}) \\ \text{s.t.} \quad & |\mathbf{F}_{\mathrm{RF}}|^2 = \frac{1}{N_{\mathrm{Tx}}}, \\ & \|\mathbf{F}_{\mathrm{RF}}\boldsymbol{f}_{\mathrm{BB},k}\|_f \le 1, \forall k = 1,2,\ldots,K. \end{aligned} \tag{6}$$

The first condition $|\mathbf{F}_{\mathrm{RF}}|^2 = \frac{1}{N_{\mathrm{Tx}}}$ in equation (6) refers to constant modulus constraint of the analog precoding, while the second condition $\|\mathbf{F}_{\mathrm{RF}}\boldsymbol{f}_{\mathrm{BB},k}\|_f \le 1$ refers to normalized power constraint.

Ⅲ. Quantum Based Approach

The quantum based approach will be introduced in this section as illustrated in Figure. 3.

3.1 QNN for Hybrid Precoding

The set of inputs for QNN are channel matrix $\mathbf{H}$ that can be generated based on an equation (2) and weight parameter θ can be obtained with random normal distribution $\mathcal{N}(0, \frac{\pi}{2})$. Every $\mathbf{h}_k$ will be inputted to QNN and outputting the row optimize of analog precoding, later will be constructed as matrix after all $\mathbf{h}_k$ already been processed through QNN. Following output from QNN $\hat{\vartheta}$ need to be converted to phase shift scale as

$$\vartheta = 2\hat{\vartheta}\pi, \tag{7}$$

Afterward, converted output ϑ will be used to calculate analog precoding[3] as follows.

$$\mathbf{F}_{\mathrm{RF}} = \frac{1}{\sqrt{N_{\mathrm{Tx}}}}e^{j\vartheta}. \tag{8}$$

Digital precoding matrix could be computed based on zero-forcing criteria according to effective channel $\bar{\mathbf{H}}$ after obtaining analog precoding $\mathbf{F}_{\mathrm{RF}}$[6] as

$$\bar{\mathbf{H}} = \mathbf{H}\mathbf{F}_{\mathrm{RF}}, \tag{9}$$

$$\hat{\mathbf{F}}_{\mathrm{BB}} = [\hat{\boldsymbol{f}}_{\mathrm{BB},1},\ldots,\hat{\boldsymbol{f}}_{\mathrm{BB},k}] = \bar{\mathbf{H}}^H(\bar{\mathbf{H}}\bar{\mathbf{H}}^H)^{-1}, \tag{10}$$

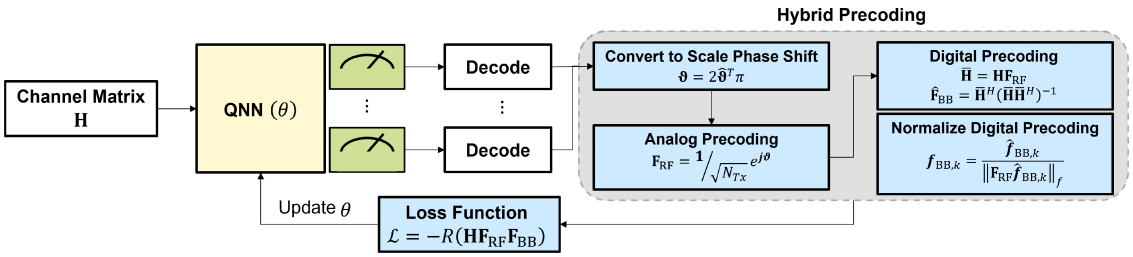

Fig. 3. Proposed Method QNN Hybrid Precoding Optimization.

normalization is needed in digital precoding to fulfill the power constraint as mentioned in equation (6). The normalization can be stated as follows.

$$\boldsymbol{f}_{\mathrm{BB},k} = \sqrt{N_{\mathrm{s}}}\frac{\hat{\boldsymbol{f}}_{\mathrm{BB},k}}{\|\mathbf{F}_{\mathrm{RF}}\hat{\boldsymbol{f}}_{\mathrm{BB},k}\|_f}, k = 1,2,...,K. \quad (11)$$

After all variables have already obtained, the calculation of the spectral efficiency can be performed based on equation (5). The loss function can be expressed as a negative number of the optimization problem $\mathscr{L}$ = -R(**H**, $\mathbf{F}_{\mathrm{RF}}$, $\mathbf{F}_{\mathrm{BB}}$) since considering unsupervised learning. Parameter shift rule[16] is employ for update gradient parameter θ, can be describe as

$$\nabla_{\theta_t}\mathscr{L} = \frac{1}{2\sinh\varepsilon}\left[\mathscr{L}(x;\theta_t+\varepsilon) - \mathscr{L}(x;\theta_t-\varepsilon)\right], \quad (12)$$

$$\theta_{t+1} = \theta_t - \eta\nabla_{\theta_t}\mathscr{L}, \quad (13)$$

where ε and η are denoted as shifting parameter and learning rate.

3.2 Quantum Circuit

Figure 4 shows the quantum circuit architecture in QNN process, there's three main parts such as input encoding, learnable parameters with entanglement layers, and measurement decoding. The operation of input encoding is mapping the classical values into superposition quantum states. Furthermore, the operation can be given as

$$U_{\mathrm{encode}}^{\boldsymbol{h}_k} : \boldsymbol{h}_k \mapsto |\boldsymbol{h}_k\rangle = \bigotimes_{i=0}^{N_{\mathrm{qubits}}} \mathbf{R}_{\mathbf{y}}(\tanh(\boldsymbol{h}_{k,i}))\mathcal{H}, \quad (14)$$

where **Ry** (·) indicate rotation on Y-axis. Also, the weight parameter θ need to be encoded from classical values into quantum states by encoding operation. The operation of encoding the weight parameter is presented as

$$U_{\mathrm{encode}}^{\theta} : \theta \mapsto |\theta\rangle = \bigotimes_{i=0}^{N_{\mathrm{qubits}}} \mathbf{R}_{\mathbf{y}}(\tanh(\theta_i)), \quad (15)$$

entanglement connecting one qubit to another can be described as $\prod_{i=0}^{N_{\mathrm{qubits}}} \mathbf{C}_{\mathbf{z}}(q_i, q_{i+1}) \otimes ... \otimes \mathbf{C}_{\mathbf{z}}(q_{N_{\mathrm{qubits}}}, q_0)$ and $\prod_{i=1}^{N_{\mathrm{qubits}}} \mathbf{C}_{\mathbf{z}}(q_{N_{\mathrm{qubits}}-i}, q_{N_{\mathrm{qubits}}-(i+1)}) \otimes ... \otimes \mathbf{C}_{\mathbf{z}}(q_1, q_0)$.

Measurement decoding is performed in the last layer to obtain the outputs of real values from quantum states into classical values with decoding operation as follows

$$\mathbf{M}_{\mathrm{QNN}} = \langle 0| U_{\mathrm{QNN}}(\boldsymbol{h}_k)^{\dagger}\mathcal{H}U_{\mathrm{QNN}}(\boldsymbol{h}_k)|0\rangle, \quad (16)$$

to reduce the error output from noisy quantum computing, the measurement is performed in N_{shot} times which is given as

$$\hat{\vartheta} \leftarrow U_{\mathrm{decode}} = \frac{1}{N_{\mathrm{shot}}}\sum_{s=1}^{N_{\mathrm{shot}}} \mathbf{M}_{\mathrm{QNN},s}, \quad (17)$$

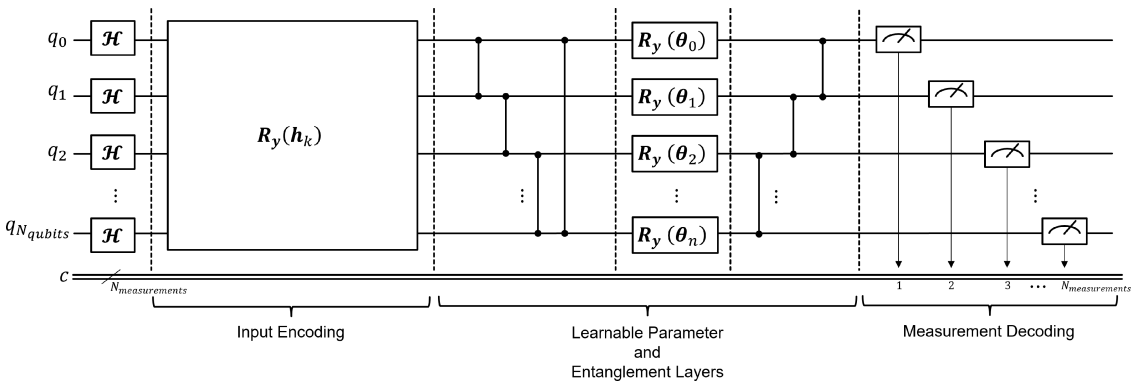

Fig. 4. Proposed quantum circuit for hybrid precoding optimization.

where N_{shot} is a number of shots taken in the quantum measurement process. Table 1 presents the quantum operations that have been used in the quantum circuit.

Table 1. Quantum Operations

Notation	Matrix
$\mathcal{H}$	$\frac{1}{\sqrt{2}}\begin{bmatrix} 1 & 1 \\ 1 & -1 \end{bmatrix}$
$\mathbf{R_y}$	$\begin{bmatrix} \cos(\frac{\theta}{2}) & -\sin(\frac{\theta}{2}) \\ \sin(\frac{\theta}{2}) & \cos(\frac{\theta}{2}) \end{bmatrix}$
$\mathbf{C_z}$	$\begin{bmatrix} 1 & 0 & 0 & 0 \\ 0 & 1 & 0 & 0 \\ 0 & 0 & 1 & 0 \\ 0 & 0 & 0 & -1 \end{bmatrix}$

Ⅳ. Experimental Results

In this section, experimental results are presented to assess the performance of QNN-based hybrid precoding for MU-MISO systems with unsupervised learning. The simulation runs in IBM Qiskit as a quantum computing platform[17] that performs the QNN operation and, ($U_{\text{encode}}^{\mathbf{h}_k}$, $U_{\text{encode}}^{\theta}$, and U_{decode}). As training parameters for QNN, can be described in Table 2. The channel matrix is generated according to equation 2 as input data.

Table 2. Training parameters

Parameters	Value
N_{TX}	4
N_{RX}	1
N_{RF}	2
N_s	2
K	2
N_{path}	10
ϕ	[0, 2π]
$N_{episode}$	20
N_{data}	200
θ	$[0, \frac{\pi}{2}]$
η	0.01
ε	$\frac{\pi}{2}$

4.1 Complexity

The complexity analysis will consider one forward propagation part and not consider the training complexity, as QNN and classical NN utilize a similar training algorithm. According to [12], the complexity of QNN and classical NN can be stated as $\mathcal{O}(N_{\text{layer}} N_{\text{neuron}})$ and $\mathcal{O}(N_{\text{layer}}(N_{\text{neuron}})^2)$ with assumption that an equal number of neurons in every layer to simplify the complexity analysis; $N_{\text{neuron}} = N_{\text{neuron}}^{(1)} = \ldots = N_{\text{neuron}}^{(N_{\text{layer}})}$.

Furthermore, the N_{neuron} for QNN is equal to number of qubits N_{qubits}, so it can be said $N_{\text{neuron}} = N_{\text{qubits}}$. As on the encoding operation, a single $\mathcal{H}$ operation yields $\mathcal{O}(1)$ and all operation of $\mathbf{R_y}(\tanh(\cdot))$ are performed simultaneously. So, $\bigotimes_{i=1}^{N_{\text{qubits}}} \mathbf{R_y}(\tanh(\mathbf{h}_{k,i}))\mathcal{H}$ yields $\mathcal{O}(1)$. The entanglement operation of the first term as $\prod_{i=0}^{N_{\text{qubits}}} \mathbf{C_z}(q_i, q_{i+1}) \otimes \ldots \otimes \mathbf{C_z}(q_{N_{\text{qubits}}}, q_0)$ yields $N_{\text{neuron}}\,\mathcal{O}(1) \approx \mathcal{O}(N_{\text{neuron}})$ and second term as $\prod_{i=1}^{N_{\text{qubits}}} \mathbf{C_z}(q_{N_{\text{qubits}}-i}, q_{N_{\text{qubits}}-(i+1)}) \otimes \ldots \otimes (q_1, q_0)$ yields $N_{\text{neuron}}\mathcal{O}(1) \approx \mathcal{O}(N_{\text{neuron}})$ as $\mathbf{Cz}(\cdot)$ operation requires $\mathcal{O}(1)$. The total complexity of entanglement can be expressed as $\mathcal{O}(N_{\text{neuron}}) + \mathcal{O}(N_{\text{neuron}}) \approx \mathcal{O}(N_{\text{neuron}})$. The measurement $\mathbf{M}_{\text{QNN}}$ requires $\mathcal{O}(N_{\text{neuron}})$ as for each measurement in qubit yields $\mathcal{O}(1)$. As for one layer, the total complexity can be defined as $\mathcal{O}(N_{\text{neuron}})$. Therefore, the total complexity can be obtained in all layers as $U_{\text{QNN}} \in \mathcal{O}(N_{\text{layer}} N_{\text{neuron}})$ for QNN.

In this paper also the number of qubits is equal to the number of transmit antenna, $N_{\text{qubits}} = N_{\text{Tx}}$. As classical NN, the N_{neuron} will equal to the number of inputs being processed $N_{\text{neuron}} = 2N_{\text{Tx}}K$. In Section 3.1, QNN needed to do K iterative to construct the optimized analog precoding matrix. Then, the total complexity of both QNN and classical NN for hybrid precoding optimization are shown in Table 3.

Table 3. Complexity comparison

Method	Complexity
QNN	$\mathcal{O}(KN_{layer}N_{\text{Tx}})$
Classical NN	$\mathcal{O}(N_{layer}\ (2N_{\text{Tx}}K)^2)$

4.2 Loss

The QNN training loss results are illustrated in

Figure 5. As shown in the figure, the loss training for QNN offers faster convergence result. On the other hand, the loss of classical NN can get more lower compared to the QNN loss result. These loss results are expected as mentioned in [12], that classical NN loss can go lower than the QNN loss result.

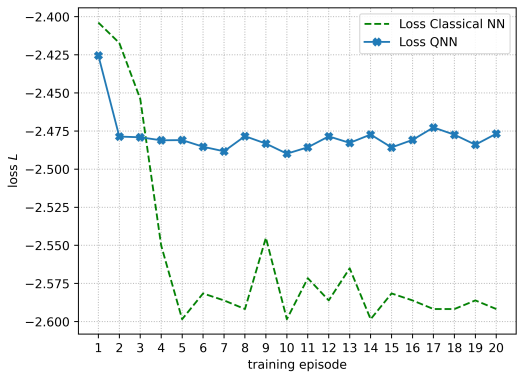

Fig. 5. Training loss progress with $\gamma = 0$ dB.

4.3 Spectral Efficiency

Figure 6 shows a comparison of the spectral efficiency from QNN-based hybrid precoding towards several hybrid precoding solutions such as classical NN, hybrid Kalman precoding algorithm [4], ZF hybrid precoding[18] and MMSE hybrid precoding[19]. The proposed method shows the best performance along with classical NN compared to the other hybrid precoding solutions and presents a high achievable spectral efficiency result while lowering the complexity. The QNN learns to maximize the construct of analog precoding and the ZF-based criteria is utilized to minimize interference of the user for digital precoding, those approaches are given an advantage for the proposed QNN hybrid precoding compared to other hybrid precoding solutions.

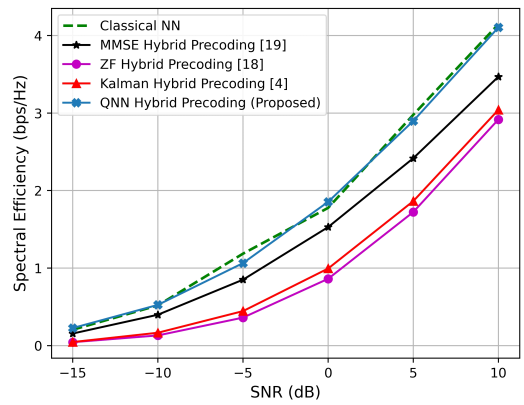

Fig. 6. Comparison of achievable spectral efficiency varying SNR with other hybrid precoding solutions. Range of γ = [-15,10] dB.

V. Conclusion

In this paper, hybrid precoding optimization based on QNN approach with unsupervised learning proposed to improve the achievable spectral efficiency performance. A channel matrix has been utilized as input data for QNN in the training process. The QNN is utilized to obtain optimal analog precoding, which is subsequently used to compute digital precoding using the zero-forcing criterion. Unsupervised learning is employed to maximize the achievable spectral efficiency performance. It's demonstrated the proposed method improves the performance result compared to other hybrid precoding solutions and maintaining the same level of result as classical NN with reducing the complexity.

The proposed method has significant potential for real-world applications in the realm of 5G and future 6G networks. This is particularly can be highlighted in high-density environments, such as urban areas and large public events, where needed short time of computation while giving the high data rates and reliable connectivity.

For future works, extension hybrid precoding for the MIMO system in QNN scheme can be considered, also adopting non-orthogonal multiple access (NOMA) can be one of technique to improve the achievable spectral efficiency. Relaxing the assumption i.e. channel perfect knowledge, can be consider as one of future direction.

References

[1] M. Xiao, S. Mumtaz, Y. Huang, et al., "Millimeter wave communications for future mobile networks," *IEEE J. Sel. Areas in Commun.*, vol. 35, no. 9, pp. 1909-1935, 2017. (https://doi.org/10.1109/JSAC.2017.2719924)

[2] O. E. Ayach, S. Rajagopal, S. Abu-Surra, Z. Pi, and R. W. Heath, "Spatially sparse precoding in millimeter wave mimo systems," *IEEE Trans. Wireless Commun.*, vol. 13, no. 3, pp. 1499-1513, 2014. (https://doi.org/10.1109/TWC.2014.011714.130846)

[3] J. Du, W. Xu, H. Shen, X. Dong, and C. Zhao, "Hybrid precoding architecture for massive multiuser mimo with dissipation: Sub-connected or fully connected structures?" *IEEE Trans. Wireless Commun.*, vol. 17, no. 8, pp. 5465-5479, 2018. (https://doi.org/10.1109/TWC.2018.2844207)

[4] A. Vizziello, P. Savazzi, and K. R. Chowdhury, "A kalman based hybrid precoding for multiuser millimeter wave mimo systems," *IEEE Access*, vol. 6, pp. 55 712-55 722, 2018. (https://doi.org/10.1109/ACCESS.2018.2872738)

[5] P. Zhang, L. Pan, T. Laohapensaeng, and M. Chongcheawchamnan, "Hybrid beamforming based on an unsupervised deep learning network for downlink channels with imperfect csi," *IEEE Wireless Commun. Lett.*, vol. 11, no. 7, pp. 1543-1547, 2022. (https://doi.org/10.1109/LWC.2022.3179362)

[6] H. Jiang, Y. Lu, X. Li, B. Wang, Y. Zhou, and L. Dai, "Attention-based hybrid precoding for mmwave mimo systems," in *2021 IEEE Inf. Theory Workshop (ITW)*, pp. 1-6, 2021. (https://doi.org/10.1109/ITW48936.2021.9611432)

[7] A. Abbas, D. Sutter, C. Zoufal, A. Lucchi, A. Figalli, and S. Woerner, "The power of quantum neural networks," *Nature Computational Sci.*, vol. 1, no. 6, pp. 403-409, Jun. 2021, ISSN: 2662-8457. (https://doi.org/10.1038/s43588-021-00084-1)

[8] S. J. Nawaz, S. K. Sharma, S. Wyne, M. N. Patwary, and M. Asaduzzaman, "Quantum machine learning for 6g communication networks: State-of-the-art and vision for the future," *IEEE Access*, vol. 7, pp. 46 317-46 350, 2019. (https://doi.org/10.1109/ACCESS.2019.2909490)

[9] M. Schuld, A. Bocharov, K. M. Svore, and N. Wiebe, "Circuit-centric quantum classifiers," *Phys. Rev. A*, vol. 101, p. 032 308, Mar. 2020. (https://doi.org/10.1103/PhysRevA.101.032308)

[10] M. Schuld, R. Sweke, and J. J. Meyer, "Effect of data encoding on the expressive power of variational quantum-machine-learning models," *Physical Rev. A*, vol. 103, no. 3, Mar. 2021, ISSN: 2469-9934. (https://doi.org/10.1103/physreva.103.032430)

[11] B. Narottama, T. Jamaluddin, and S. Y. Shin, "Quantum neural network with parallel training for wireless resource optimization," *IEEE Trans. Mobile Comput.*, vol. 23, no. 5, pp. 5835-5847, 2024. (https://doi.org/10.1109/TMC.2023.3321467)

[12] B. Narottama and S. Y. Shin, "Quantum neural networks for resource allocation in wireless communications," *IEEE Trans. Wireless Commun.*, vol. 21, no. 2, pp. 1103-1116, 2022. (https://doi.org/10.1109/TWC.2021.3102139)

[13] T. Jamaluddin, B. Narottama, and S. Y. Shin, "Quantum deep unfolding based resource allocation optimization for future wireless networks," *J. KICS*, vol. 48, no. 8, pp. 897-905, 2023. (https://doi.org/10.7840/kics.2023.48.8.897)

[14] A. Alkhateeb, O. El Ayach, G. Leus, and R. W. Heath, "Channel estimation and hybrid precoding for millimeter wave cellular systems," *IEEE J. Sel. Topics in Signal Proc.*, vol. 8, no. 5, pp. 831-846, 2014. (https://doi.org/10.1109/JSTSP.2014.2334278)

[15] X. Wei, C. Hu, and L. Dai, "Deep learning for beamspace channel estimation in millimeterwave massive mimo systems," *IEEE Trans. Commun.*, vol. 69, no. 1, pp. 182-193, 2021. (https://doi.org/10.1109/TCOMM.2020.3027027)

[16] M. Schuld, V. Bergholm, C. Gogolin, J. Izaac,

and N. Killoran, “Evaluating analytic gradients on quantum hardware,” *Phys. Rev. A*, vol. 99, p. 032 331, Mar. 2019. (https://doi.org/10.1103/PhysRevA.99.032331)

[17] G. Aleksandrowicz, T. Alexander, P. Barkoutsos, et al., *Qiskit: An Open-source Framework for Quantum Computing*, version 0.7.2, Feb. 2019. (https://doi.org/10.5281/zenodo.2562111)

[18] A. Alkhateeb, G. Leus, and R. W. Heath, “Limited feedback hybrid precoding for multi-user millimeter wave systems,” *IEEE Trans. Wireless Commun.*, vol. 14, no. 11, pp. 6481-6494, 2015. (https://doi.org/10.1109/TWC.2015.2455980)

[19] D. H. N. Nguyen, L. B. Le, and T. Le-Ngoc, “Hybrid mmse precoding for mmwave multiuser mimo systems,” in *2016 IEEE Int. Conf. Commun.* (*ICC*), pp. 1-6, 2016. (https://doi.org/10.1109/ICC.2016.7510844)

Adriansyah Dwi Rendragraha

Aug. 2017 : B.S. degree, School of Computing, Telkom University, Bandung, Indonesia.

Sept. 2022~Current : M.Eng. student, Dept. of IT Convergence Engineering, Kumoh National Institute of Technology, Gumi, South Korea.

<Research Interest> Artificial Intelligence, Machine Learning, Natural Language Processing, Quantum Neural Network, Hybrid Precoding.

[ORCID:0009-0000-6328-0351]

Soo Young Shin

Feb. 1999 : B.Eng. degree, School of Electrical and Electronic Engineering, Seoul National University

Feb. 2001 : M.Eng. degree, School of Electrical, Seoul National University

Feb. 2006 : Ph.D. degree, School of Electrical Engineering and Computer Science, Seoul National University

July 2006~June 2007 : Post Doc. Researcher, School of Electrical Engineering, University of Washington, Seattle, USA.

2007~2010 : Senior Researcher, WiMAX Design Laboratory, Samsung Electronics, Suwon, South Korea

Sept. 2010~Current : Professor, School of Electronic Engineering, Kumoh National Institute of Technology

<Research Interest> 5G/6G wireless communications and networks, signal processing, the Internet of Things, mixed reality, and drone applications.

[ORCID:0000-0002-2526-2395]